Concentration dependence of structural and dynamical quantities in colloidal aggregation: Computer simulations

Mohammed Lach-hab,[1] Agustín E. González,[2] and Estela Blaisten-Barojas[1]
[1]*Institute for Computational Sciences and Informatics, George Mason University, Fairfax, Virginia 22030*
[2]*Instituto de Física, Universidad Nacional Autónoma de México, Apartado Postal 20-364, 01000 México, Distrito Federal*
(Received 15 March 1996; revised manuscript received 18 July 1996)

We have performed extensive numerical simulations of diffusion-limited (DLCA) and reaction-limited (RLCA) colloid aggregation to obtain the dependence on concentration of several structural and dynamical quantities, among them the fractal dimension of the clusters before gelation, the average cluster sizes, and the scaling of the cluster size distribution function. A range in volume fraction ϕ spanning two and a half decades was used for this study. For DLCA, a square root type of increase of the fractal dimension with concentration from its zero-concentration value was found: $d_f = d_f^0 + a\phi^\beta$, with $d_f^0 = 1.80 \pm 0.01$, $a = 0.91 \pm 0.03$, and $\beta = 0.51 \pm 0.02$. For RLCA the same type of behavior was found, this time with $d_f^0 = 2.10 \pm 0.01$, $a = 0.47 \pm 0.03$, and $\beta = 0.66 \pm 0.08$. In the case of DLCA, the exponent z that defines the power law increase of the weight-average cluster size (S_w) with time also increases as a square root type with concentration: $z = z^0 + b\phi^\alpha$, with $z^0 = 1.07 \pm 0.06$, $b = 3.09 \pm 0.22$, and $\alpha = 0.55 \pm 0.03$, while the exponent z' that describes the power law increase of the number-average cluster size (S_n) with time follows the same law: $z' = z'^0 + b'\phi^{\alpha'}$, now with $z'^0 = 1.05 \pm 0.04$, $b' = 3.41 \pm 0.24$, and $\alpha' = 0.46 \pm 0.02$. We have also found that the cluster size distribution function scales as $N_s(t) \approx N_0 S_w^{-2} f(s/S_w)$, where N_0 is the number of initial colloidal particles and f is a concentration-dependent function displaying an asymmetric bell shape in the limit of zero concentration. For RLCA, we found an exponential increase of the average cluster sizes for a substantial range of the aggregation time: $S_w \sim e^{p\phi t}$ and $S_n \sim e^{q\phi t}$, with $p \approx 2q$. For longer times the behavior departs from the exponential increase and, in the case of S_w for low concentration, it crosses over to a power law increase. In the RLCA case the scaling is as in DLCA where now a power law decay of the function f defines the exponent τ, $f(x) \sim x^{-\tau} g(x)$, with $g(x)$ decaying exponentially fast for $x > 1$. A slight dependence of the exponent τ on concentration was computed around to the value $\tau = 1.5$. [S1063-651X(96)10311-1]

PACS number(s): 64.60.Qb, 02.70.−c, 05.40.+j, 81.10.Dn

I. INTRODUCTION

Significant advances in the understanding of irreversible kinetic colloid aggregation have been made in the past decade [1,2]. For a wide range of experimental systems the bonds formed between the colliding particles are very strong, inhibiting the rearrangement of the particles within the clusters. This mechanism produces opened clusters that exhibit fractal structure [3]. That is, the exponent d_f that relates the total mass M of the aggregate to its typical size is not an integer: $M \sim R^{d_f}$. This peculiar discovery of the scale invariance of the clusters [4–8] promoted great interest and work in the study of these systems.

Two limiting regimes of the aggregation processes were subsequently identified [9–12]. There is a rapid regime which is diffusion limited [diffusion-limited colloid aggregation (DLCA)], characterized by $d_f \approx 1.8$, for which the colliding particles stick at first contact. If the aggregation is much slower, due to a very small sticking probability, the system reaches a different and opposed regime which is reaction limited [reaction-limited colloid aggregation (RLCA)] leading to more compact clusters ($d_f \approx 2.1$). This result can be rationalized by noting that the colliding clusters interpenetrate more if the sticking probability is close to zero. In addition, researchers found that aggregating systems possess not only spatial scaling but also dynamic scaling behavior [13–17]. For DLCA, the two already known dynamic results are as follows. (i) There is a power law growth of the average cluster sizes (S_n and S_w) defined by the exponent z: S_n, $S_w \sim t^z$. It was experimentally found that z was approximately one. (ii) The cluster size distribution function shows the scaling behavior $N_s(t) \approx N_0 S(t)^{-2} f[s/S(t)]$, where $S(t)$ is equal to the number-average or weight-average cluster size and f is a universal function, bell shaped when plotted as function of s on a log-log scale. On the other hand, in the limit of RLCA researchers found (i) an exponential increase of the mean cluster sizes with time such that $S_w(t) \sim S_n^2(t)$ and (ii) a scaling similar to that for DLCA in which $S(t)$ is the weight-average cluster size. The function f in this case is a universal function with power law decay $f(x) \sim x^{-\tau} g(x)$, where $g(x)$ decays exponentially fast for $x > 1$ and $\tau = 1.5$. All these facts have been confirmed extensively, both experimentally [10–12,15,16,18–26] and with computer simulations [2,5,6,27–30]. It is important to emphasize that the above results, mainly the experimental ones, have been obtained for a low volume fraction regime and researchers sometimes extrapolate them thinking that they apply to high concentrations as well. Thinking it over, one cannot escape the conclusion of a concentration dependence of the previously described quantities. Take, for example, the fractal dimension. In a very concentrated regime the small clusters are already interpenetrated before sticking and when they stick, they do so not at the tips of their longer arms but also in the middle. Therefore the compactness of the clusters should in-

crease with concentration and hence the fractal dimension should increase. Concentration changes become important in the laboratory and in industrial applications.

Two attempts to calculate this dependence in the DLCA limit have been reported recently for a two-dimensional system of hard disks [31] and for a two-dimensional square lattice [32]. van Garderen *et al.* [31] compute numerically a short range fractal dimension of two-dimensional blobs composing a single final aggregate. This fractal dimension is obtained from the decay of the scattering function $S(q)$, for a q range corresponding to distances of four disk diameters up to a concentration-dependent coherence length ξ. Their reported value of $d_f \sim 1.45$ is independent of concentration. However, the same authors also report a long range fractal dimension that changes smoothly between 1.45 and 2, for the remaining range beyond the coherence length and up to the size of the aggregate. In this case they obtain a concentration-dependent fractal dimension that tends to 2 for high concentrations, when there are many *terminal blobs* [33,34] in the reaction box. This is indeed to be expected because the system looks homogeneous at long lengths. To obtain a long range fractal dimension smaller than 2 for intermediate concentrations is an artifact. As calculated, this fractal dimension is just a crossover value that would tend to 2 if the authors had used a much larger computational box, capable of containing many more terminal blobs [33,34]. Pencea and Dumitrascu [32] obtained a concentration-dependent fractal dimension for the aggregating clusters before gelation that changed its value from 1.5 to 1.9, for concentrations between 0.1 and 0.5. However, no discussion on the statistics of their calculations was published, making it difficult to assess the significance of their results.

The calculations of van Garderen *et al.* and Pencea and Pumitrascu are different because different fractal dimensions were calculated. In addition, the diffusivity of the growing clusters is correctly addressed only in the calculation of Pencea and Dumitrascu. In this regard one should note that by moving all the clusters simultaneously the same step length as in Ref. [31], the same diffusivity is assigned to a monomer as to a very big cluster. Although this mistake may not affect structural quantities such as the fractal dimension, it would certainly make a difference in the evaluation of dynamic quantities such as the cluster size distribution function.

The only published work in three dimensions known to the authors, addressing a concentration dependence of fractal dimensionalities, is that of Hasmy and Jullien [35]. In this work, as in Ref. [31], the short range fractal dimension of small blobs in a gelling network is calculated from the decay of the pair correlation function: $g(r,t) \sim r^{d_f - 3}$, for $3 < r < \xi$. These authors find an increase of this short range fractal dimension with concentration. This is in opposition to the two-dimensional work of van Garderen *et al.* [31].

In this work we present results from extensive numerical simulations for the concentration dependence of several structural and dynamical quantities obtained for three-dimensional aggregation processes in the flocculation regime. The algorithms used have already been applied with success to demonstrate dynamic scaling in computer simulations of these systems [29,30], as well as to predict the scaling of the structure factor [33,34]. These algorithms allow us to obtain the fractal characteristics of individual clusters extracted from the reaction bath where the aggregation is taking place, *before* gelation occurs. Experimentally such a situation can be achieved by diluting repeatedly the bath where the reaction takes place [12,26]. Our computational approach is related to that of Ref. [32] and superior to that of Ref. [31] for the calculation of dynamical quantities because the correct diffusivity is given to clusters of different masses at changing concentration. This work is a calculation in three dimensions of the concentration dependence of *both* structural and dynamic quantities in the DLCA and RLCA limits. We emphasize that the fractal dimension calculated in this work refers to that of *individual* clusters in the flocculation regime, i.e., before gelation. It may not necessarily coincide with that of Ref. [35] associated to the blobs embedded in an infinite gel.

The organization of this article is as follows. Section II describes the algorithm used to perform the simulations and the methodology used to obtain the structural and dynamical quantities. Sections III–V present the concentration dependence of these properties in both limits, DLCA and RLCA. Section III describes the calculation of the fractal dimension of the growing clusters before gelation. Section IV pertains to the exponents z and z' that characterize the power law time behavior of S_w and S_n. This section addresses also the exponential growth observed during the early stages of the aggregation time. Section V describes the scaling that results from the dynamical behavior of the growing clusters. Section VI summarizes the results with final remarks about their validity.

II. THE MODEL AND THE METHOD

In this work we use a cubic lattice model where the lattice cells may be occupied by colloidal particles. Although continuum models can be developed [36], the algorithm used here has the convenience of its execution speed, particularly when using a large number of particles. Initially all the colloidal particles are randomly distributed and unaggregated although some of them may touch each other at some points. At a given intermediate time we have a collection of clusters made of nearest-neighbor occupied lattice cells that are diffusing randomly. One of these clusters is picked at random and moved by one lattice unit in a random direction if a random number X uniformly distributed in the range $0 < X < 1$ satisfies the condition $X < D(s)/D_{\max}$, where $D(s) \sim s^{-1/d_f}$ is the diffusion coefficient for the selected cluster of size s and $D_{\max}$ is the maximum diffusion coefficient for any cluster in the system. Otherwise the cluster is not moved. In the previous expression d_f is the fractal dimension of the clusters. Once a cluster is selected the time is increased by $1/(N_c D_{\max})$, where N_c is the number of clusters in the system at that time independently of whether the cluster is actually moved or not. An encounter is defined by an attempt of one moving cluster to overlap the lattice cells occupied by another. In this case the move is not allowed and the moving cluster either sticks (and is merged) to the other with probability P_0 or remains side by side to the other with probability $1 - P_0$. The values used for P_0 were one for the DLCA case and 0.0005 for RLCA. This last value is small enough to successfully show dynamic scaling in

RLCA [30]. The simulation is terminated just before the gelation point.

During the simulations we recorded for selected physical times the following dynamical quantities: (1) the total number of clusters, from which we were able to obtain the number-average cluster size; (2) the weight-average cluster size; (3) the cluster size distribution; and (4) the radius of gyration versus the number of monomers for every (all of the) clusters formed during the simulation.

Various strategies were employed to deal with the concentration dependence of the fractal dimension to account for the diffusivity of the clusters $D(s) \sim s^{-1/d_f}$. A set of 20 calculations of the fractal dimension for every concentration studied was performed, using the accepted value $d_f = 1.8$ for DLCA (2.1 for RLCA) to measure the cluster diffusivity. The best analytical fit to a calculated concentration-dependent fractal dimension was obtained. From this fit we extracted *first order* values of the fractal dimension $d_f(\phi)$ at each concentration and input them to account for the changes in cluster diffusivity. A set of 40 simulations (up to 100 for large concentrations) was performed—called the output simulations—and these are the results reported in this paper.

In addition, for some concentrations we performed a self-consistent calculation of the fractal dimension. An initial d_f was used to calculate $D(s)$. At the end of the first simulation a new d_f was calculated, which was then input as an initial value to calculate $D(s)$ in a second simulation. The process was repeated up to 40 iterations per concentration. This method does not converge to a value of d_f more accurate than what we report in this paper. In all cases the self-consistent values were within the standard deviation of the sample of simulations reported in this paper.

The following 14 volume fractions were considered in DLCA: 0.001, 0.003, 0.0055, 0.01, 0.03, 0.072, 0.1, 0.139, 0.2, 0.24, 0.3, 0.4, 0.469, and 0.5. In the RLCA case a total of 15 were used: 0.003, 0.0055, 0.01, 0.03, 0.06, 0.072, 0.1, 0.139, 0.170, 0.2, 0.24, 0.3, 0.4, 0.469, and 0.5. In DLCA for each concentration up to 0.01 a total of 40 output simulations were performed whereas for each concentration above 0.01 a total of 100 output simulations were carried out. In the RLCA case for each concentration up to 0.01 a total of 20 output simulations were performed and for the other concentrations a total of 40 output simulations per concentration were carried out except for $\phi = 0.469$ and 0.5 where 80 and 100 output simulations were performed, respectively. Each simulation in both DLCA and RLCA contains on the order of 30 000 initial monomers. This number of particles is large enough to allow for a meaningful statistical analysis.

We should note that these calculations are extremely computer intensive. DLCA calculations are 450 times faster than RLCA. For example, one simulation at a concentration of $\phi_a = 0.17$ requires a CPU time $t_{\mathrm{CPU}_a} = 12$ sec for DLCA and 90 min for RLCA in a dedicated MIPS R4400 200 MHz IP22 processor. The computation time for another simulation at a different concentration ϕ scales up to $t_{\mathrm{CPU}_a}\phi_a/\phi$. All together, the results reported in this paper constitute an accomplished challenging computer effort.

III. THE FRACTAL DIMENSION

A. DLCA

For each of the 40 (100 upon the case) output simulations of each concentration the value of the fractal dimension was obtained from the log-log plots of the radius of gyration versus size of all the clusters formed during the whole aggregation time. Very small clusters were neglected in this analysis such as to cover only the asymptotic regime of large clusters (greater than 50 monomers). Subsequently, we averaged the 40 (100 upon the case) values of the fractal dimension for each concentration and plotted these averages versus the concentration (volume fraction) ϕ. In Fig. 1(a) the points correspond to the 14 averages and the vertical bars show twice the standard deviation (96% confidence).

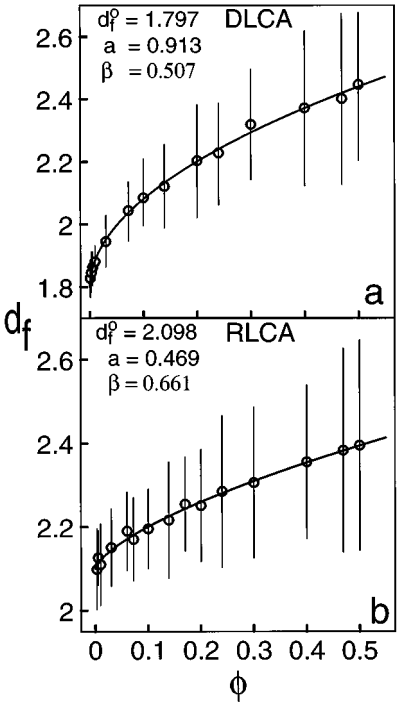

FIG. 1. The fractal dimension as a function of volume fraction. (a) DLCA case: for each of the concentrations studied, averages are over 40 simulations for $\phi \leqslant 0.1$ and over 80 simulations for $\phi > 0.1$. (b) RLCA case: averages are over 20 simulations for $\phi \leqslant 0.1$ and over 40 simulations for $\phi > 0.1$. Solid lines correspond to the fit $d_f = d_f^0 + a\phi^\beta$. Error bars represent twice the standard deviation.

Nothing prevents our algorithm from being used for high concentrations near $\phi = 1$. However, we choose to work below and a little above the percolation threshold $\phi_c = 0.312$ [37] for our simple cubic lattice model to ensure that the initial clusters of cubic monomers are separated. Therefore our results are valid for small and intermediate concentrations $\phi \leqslant 0.5$. Higher concentrations of $\phi \to 1$ are outside the scope of this work.

Within the valid range of concentrations, the best functional fit yielded a square root type of increase of the fractal dimension from its zero concentration value. Namely, $d_f = d_f^0 + a\phi^\beta$, where $d_f^0 = 1.797 \pm 0.011$, $a = 0.913 \pm 0.025$, $\beta = 0.507 \pm 0.022$. Errors correspond to twice the standard deviation of the nonlinear fit. It is important to emphasize that 1.797, the intersect at $\phi = 0$, is the accepted value of the DLCA fractal dimension $d_f \approx 1.8$ in the dilute limit.

B. RLCA

A procedure similar to that in DLCA was followed to obtain the fractal dimension in RLCA. Only concentrations

below or close to the percolation threshold were considered and small clusters were neglected when calculating the fractal dimension. Figure 1(b) shows the fractal dimension as a function of concentration where each of the 15 points corresponds to the average over the output simulations. As in the DLCA case we find that, within the valid range of concentrations, the best functional fit yields a square root type of increase of the fractal dimension: $d_f = d_f^0 + a\phi^\beta$, where $d_f^0 = 2.098 \pm 0.010$, $a = 0.469 \pm 0.025$, and $\beta = 0.661 \pm 0.080$. Once again, the value of d_f^0 is very close to the RLCA accepted fractal dimension in the dilute limit (≈ 2.1).

Although the same square root behavior as in the DLCA case was observed for RLCA, the error on the best estimated parameters is larger. This is expected because during the RLCA aggregation the morphology of the growing clusters is richer than in DLCA.

IV. TIME BEHAVIOR OF THE AVERAGE CLUSTER SIZE

A. DLCA and the exponents z and z'

The time behavior of both the average cluster size S_n and of the weighted average S_w is seen to be exponential at the early stages of the growth process. In DLCA in less than one-thousandth of the total aggregation time the system crossed over to a power law growth defined by the exponent z for S_w and z' for S_n:

$$S_w(t) \sim t^z, \quad S_n(t) \sim t^{z'}. \tag{1}$$

The methodology to obtain the exponents z and z' is summarized elsewhere [30,36]. We located the time interval within which there is a linear behavior in the log-log plots of S_w and S_n versus time. Within this time interval we fit a straight line to obtain the above defined exponents. The time region in which the fit is performed is bounded from below by the crossover from the exponential behavior and from above by noise due to finite size effects. As the concentration increases, this time region decreases and eventually disappears, marking a concentration threshold above which it is not possible to find these exponents, at least for our finite lattice simulations.

In Fig. 2(a) we show the averages of the exponents z and z' over the output simulations plotted as a function of concentration. For concentrations larger than $\phi = 0.24$ for S_w and larger than $\phi = 0.072$ for S_n, it was not possible to find a straight line regime in the log-log plots. Figure 2(a) reflects this fact.

The best functional fit gives a square root type of dependence of these exponents with concentration. We fitted the exponent z to the function $z = z^0 + b\phi^\alpha$ and the exponent z' to the function $z' = z'^0 + b'\phi^{\alpha'}$, obtaining $z^0 = 1.067 \pm 0.056$, $b = 3.088 \pm 0.216$, $\alpha = 0.547 \pm 0.034$, $z'^0 = 1.045 \pm 0.039$, $b' = 3.413 \pm 0.245$, and $\alpha' = 0.465 \pm 0.020$. It is important to note that the calculated values for z^0 and z'^0 are quite close to unity, which is the accepted value in the dilute limit.

B. RLCA and the exponential growth

As already mentioned, the plots of S_w versus time present a crossover from an exponential increase to a power law behavior at a sufficiently long time. However, in RLCA we found that the exponential behavior is clearly observed for a much longer fraction of the whole aggregation time and that the region of validity of the power law is noticeable only at low concentrations and at times three decades longer than in DLCA. For the average cluster size S_n, it was not possible to obtain the exponent z' even at low concentrations, due to the absence of a straight line regime in the log-log plots.

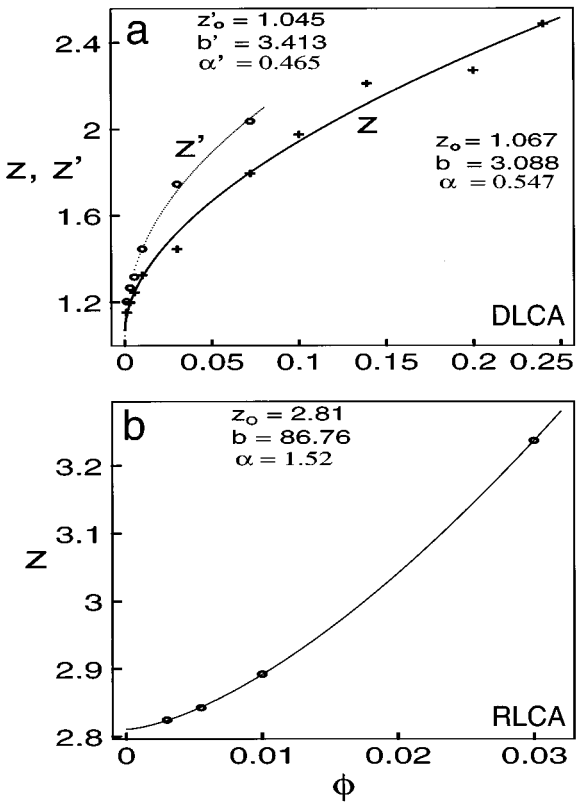

FIG. 2. The exponents z and z' vs volume action ϕ for concentrations where it is possible to define a region of linear behavior in the log-log plots of S_w and S_n vs time. (a) DLCA case: averages are over 40 simulations. (b) RLCA case: averages are over 20 simulations. The solid and dotted lines depict the functional fit $z = z^0 + b\phi^\alpha$ and $z' = z'^0 + b'\phi^{\alpha'}$, respectively.

Figure 2(b) shows the averages over 20 output simulations of the z exponent as a function of concentration only for those concentrations where we could obtain it ($\phi = 0.003$, 0.0055, 0.01, and 0.03). The best functional fit (continuous curve) gives $z = z_0 + b\phi^\alpha$, where $z_0 = 2.811 \pm 0.001$, $b = 86.76 \pm 0.42$, and $\alpha = 1.516$. Although there are just four points and we cannot be conclusive, the concentration dependence of the exponent z at low concentrations in RLCA seems to be very different than in DLCA, showing a steeper increase.

The exponential increase of the mean cluster sizes for a respectable portion of the total aggregation time was particularly noticeable for the high concentration simulations. In Fig. 3 the $\ln S_w$ is plotted as a function of time for the output simulations at three concentrations: (a) $\phi = 0.003$, (b) $\phi = 0.072$, and (c) $\phi = 0.3$. The time range shown in the figures covers the total aggregation time before the gelation point. Results for S_n are quite similar to those for S_w illustrated in Fig. 3. From graphs of $\ln S_n$ and $\ln S_w$ as a function of time we calculated the constant that multiplies the time in

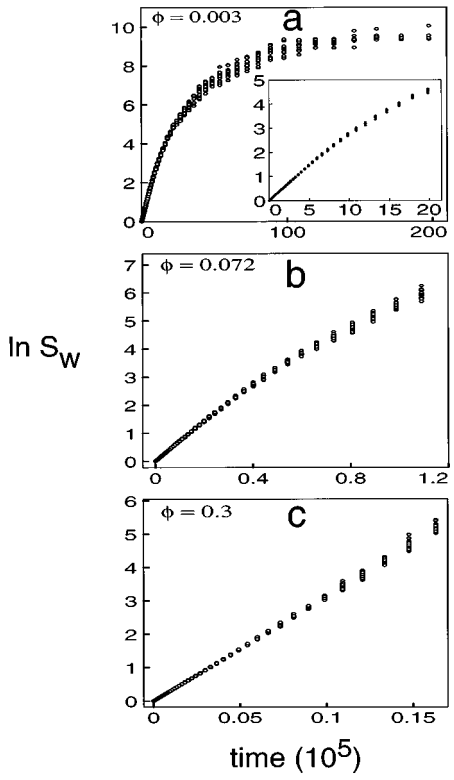

FIG. 3. RLCA case. The $\ln S_w(t)$ vs time behavior during the whole aggregation process before gelation for 20 simulations at each concentration: (a) $\phi=0.003$, (b) $\phi=0.072$, and over 40 simulations for (c) $\phi=0.3$. Time is in reduced units.

the exponential growth (the slope m for S_w and m' for S_n of the straight lines) and plot them versus concentration. Figure 4 shows the concentration dependence of m and m'. These plots reveal a clear linear dependence, i.e., $m=p\phi$ and $m'=q\phi$. The values obtained for p and q were $p=0.001\,019 \pm 0.000\,024$ and $q=0.000\,508\pm0.000\,008$. The fact that $p\approx 2q$ indicates that $S_w\sim S_n^2$ at least for a good initial part of the aggregation time. In conclusion, these results can be concisely written as follows:

$$S_w\sim e^{p\phi t}, \quad S_n\sim e^{q\phi t}, \tag{2}$$

with $p\approx 2q$.

V. THE SCALING

A. DLCA

We tested several scaling equations for the cluster size distribution function. Our first attempt was the scaling proposed in Ref. [38]: $N_s(t)\approx N_0 s^{-2} f(s/S_w)$. Using this formula it was not possible to collapse the data for different times during the aggregation into one single master curve. The second attempt was the formula given in Refs. [12,26]: $N_s(t)\approx N_0 S_n^{-2} f(s/S_n)$. In this case we were able to collapse the data only for the simulations at low concentration. Finally we tried the form $N_s(t)\approx N_0 S_w^{-2} f(s/S_w)$, for which we were able to fully collapse the data for all concentrations. The exponent of S_w that best correlated the data was about -2.

The fact that the formula in Refs. [12,26] gave scaling at low concentrations is apparently related to the behavior of the exponents z and z'. At low concentrations $z=z'=1$ and S_n is proportional to S_w. However, at finite concentrations $z\neq z'$ and the cluster size averages are not proportional. Hence, if scaling works with one of them, it cannot work with the other.

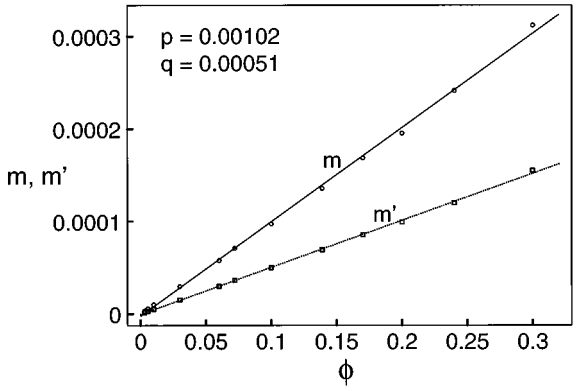

FIG. 4. RLCA case. Concentration dependence of the slopes m and m' of the straight lines in the plots of $\ln S_w$ and $\ln S_n$ vs time.

It is important to mention that the shape of the scaling function is concentration dependent. For low concentrations the shape is asymmetrically bell shaped as in Refs. [12,26]. However, with increasing concentration the left branch of the curve tends to rise, becomes flat for $\phi\approx 0.03$, and has a negative slope for higher concentrations. Figures 5 shows the master curves for three concentrations: (a) $\phi=0.001$, (b) $\phi=0.03$, and (c) $\phi=0.139$, where data from all the output simulations were considered.

B. RLCA

To scale the data for the cluster size distribution function, we corroborated [12,26,30] that the form $N_s(t) \approx N_0 S_w^{-2}(t) f(s/S_w(t))$ that we found valid for the DLCA case is also valid here. However, the function $f(x)$ is no longer bell shaped and has a power law decay defined by the exponent τ: $f(x)\sim x^{-\tau} g(x)$. Here $g(x)$ is a cutoff function decaying exponentially fast for $x>1$. As in the DLCA case to fully collapse the data we needed to exponentiate S_w to a power of approximately -2. A slight dependence of the exponent τ on concentration was found ranging from 1.37 for low concentrations up to 1.62 for very high concentrations. This can be a real effect or can be an artifact of the computational algorithm which takes into account most of the mechanisms experienced by the real aggregating particles but not all of them. That the dependence on concentration is very slight together with the available experimental data and theoretical results (which propound a constant τ value of 1.5 [11,12,15,21,23,26,39]) may indicate the second possibility to be more likely. A possible explanation may be the fact that, in the simulation, data for large clusters are scarce (left of the master curves) due to the finite size of the computational cell whereas the experimental data refer to infinite [12,26] material. Figures 6(a) and 6(b) illustrate $\ln[S_w^{2.1}(t) N_s(t)/N_0]$ versus $\ln[s/S_w(t)]$ for $\phi=0.003$ and 0.072, respectively. In Fig. 6(c), for $\phi=0.3$, it was necessary to exponentiate S_w to the power 2.2 to obtain the best collapse of the data. As in DLCA, figures display data for the numbers of clusters coming from all the output simulations for each concentration.

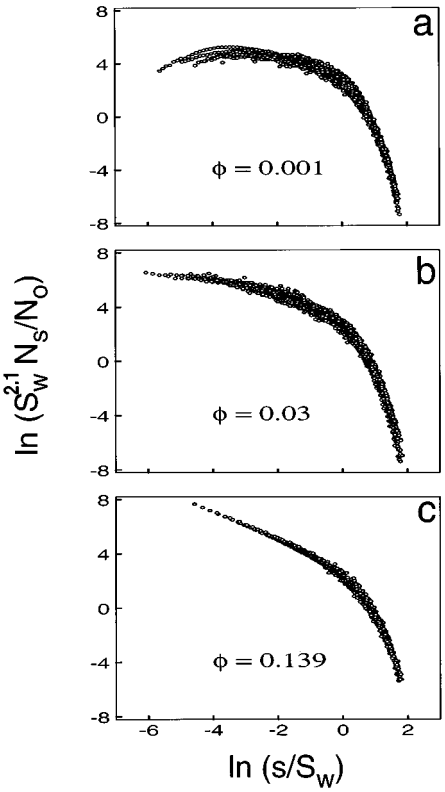

FIG. 5. DLCA case of $\ln[S_w^{2.1}(t)N_s(t)/N_0]$ vs $\ln[s/S_w(t)]$ for (a) ϕ=0.001, (b) ϕ=0.03, and (c) ϕ=0.139. The cluster numbers function $N_s(t)$ contains data from 40 simulations at ϕ=0.001, 0.03, and from 80 simulations at ϕ=0.139. $S_w(t)$ is the average over those simulations. Sizes are in reduced units.

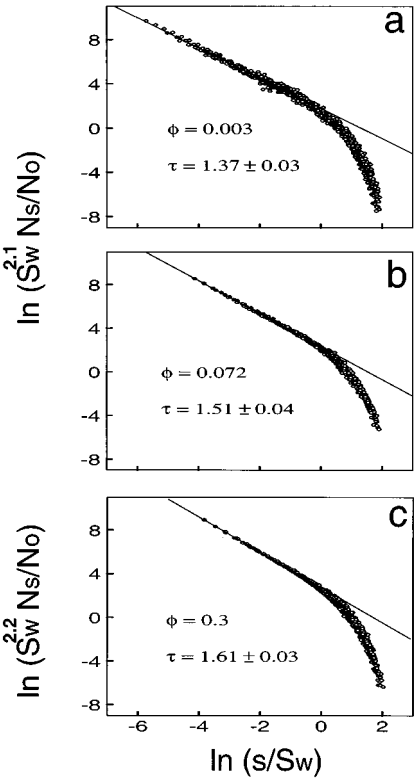

FIG. 6. RLCA case of $\ln[S_w^{2.1}(t)N_s(t)/N_0]$ vs $\ln[s/S_w(t)]$. The cluster number function $N_s(t)$ contains data from 20 simulations at each concentration (a) ϕ=0.003, (b) ϕ=0.072, and from 40 simulations at (c) ϕ=0.3. $S_w(t)$ is the average over those simulations. For ϕ=0.3 it was necessary to exponentiate S_w to the power 2.2 to obtain the best possible collapse. Sizes are in reduced units.

VI. SUMMARY AND CONCLUSIONS

We have seen a real effect in the concentration dependence of the structural and dynamical quantities in colloid aggregation manifested by an increase of these quantities when increasing the concentration. In particular, the fractal dimension of the clusters increases at higher concentrations. As shown in this work, in DLCA the fractal dimension at around ϕ=0.05 overcomes the value of 2, which is the fractal dimension of percolation clusters below the percolation threshold of ϕ_c=0.312. This suggests different universality classes for both processes.

The fact that the z exponents increase with concentration is a consequence that the aggregating particles and clusters travel shorter distances to meet and eventually stick to each other as the concentration is increased. Therefore the system should take less time to aggregate and hence the mean cluster sizes should increase faster at higher concentrations. For this same reason for the RLCA case the factor that multiplies the time in the exponential increase should increase with concentration.

A word of caution needs to be said before trying to apply these results to experimental systems. In our algorithm, the volume fraction is defined as the fraction of cells of the lattice occupied by colloidal particles. In a real system, the volume fraction is defined as the volume occupied by the colloidal particles divided by the total volume of the system. It is not evident how to relate one volume fraction to the other. The belief is that they are proportional to each other. This would fully validate the results in this work and only minor changes in the constants that multiply the volume fractions in the above formulas would need to be introduced in order to compare with experiments.

We finally need to mention that the increase in the fractal dimension with increasing concentration occurs when the computation of d_f is performed in real space, that is, directly from the relation between the mass and radius of gyration of an aggregate: $M \sim R^{d_f}$ as in our calculations. However, if the evaluation of d_f is made in q space, like from the high-q decay of the structure factor: $S(q) \sim q^{-d_f}$, an opposite trend of decreasing fractal dimension with increasing concentration has been reported [24,34,35]. Notwithstanding that this result in the literature needs to be validated and explained, we believe that the *true* fractal dimension is the one that relates the mass and radius of the aggregate when both quantities are obtained in real space.

ACKNOWLEDGMENTS

E.B.B. acknowledges support from NSF Grant No. INT-9502985 for international travel and from the Institute for Computational Sciences and Informatics for providing support to M.L. and for the extensive CPU use of the cluster of workstations. A.E.G. acknowledges support from CONACYT Grant Nos. 4906-E and E120.1381.

[1] *Kinetics of Aggregation and Gelation*, edited by F. Family and D. P. Landau (Elsevier, Amsterdam, 1984).
[2] T. Vicsek, *Fractal Growth Phenomena* (World Scientific, Singapore, 1989).
[3] B. B. Mandelbrot, *The Fractal Geometry of Nature* (Freeman, San Francisco, 1982).
[4] S. R. Forrest and T. A. Witten, J. Phys. A **12**, L109 (1979).
[5] P. Meakin, Phys. Rev. Lett. **51**, 1119 (1983).
[6] M. Kolb, R. Botet, and R. Jullien, Phys. Rev. Lett. **51**, 1123 (1983).
[7] D. A. Weitz and M. Oliveria, Phys. Rev. Lett. **52**, 1433 (1984).
[8] D. W. Schaefer, J. E. Martin, P. Wiltzius, and D. S. Cannell, Phys. Rev. Lett. **52**, 2371 (1984); in *Kinetics of Aggregation and Gelation* (Ref. [1]), p. 185.
[9] D. A. Weitz and J. S. Huang, in *Kinetics of Aggregation and Gelation* (Ref. [1]), p. 19.
[10] D. A. Weitz, J. S. Huang, M. Y. Lin, and J. Sung, Phys. Rev. Lett. **54**, 1416 (1985).
[11] M. Y. Lin, H. M. Lindsay, D. A. Weitz, R. C. Ball, R. Klein, and P. Meaking, Nature (London) **339**, 360 (1989).
[12] M. L. Broide and R. J. Cohen, Phys. Rev. Lett. **64**, 2026 (1990).
[13] T. Vicsek and F. Family, Phys. Rev. Lett. **52**, 1669 (1984).
[14] M. Kolb, Phys. Rev. Lett. **53**, 1653 (1984).
[15] D. A. Weitz and M. Y. Lin, Phys. Rev. Lett. **57**, 2037 (1986).
[16] E. Pefferkorn, C. Pichot, and R. Varoqui, J. Phys. (Paris) **49**, 983 (1988).
[17] P. G. J. van Dongen and M. H. Ernst, J. Phys. A **18**, 2779 (1985).
[18] C. Aubert and D. S. Cannell, Phys. Rev. Lett. **56**, 738 (1986).
[19] G. Bolle, C. Cametti, P. Codastefano, and P. Tartaglia, Phys. Rev. A **35**, 837 (1987).
[20] F. Ferri, M. Giglio, E. Paganini, and U. Perini, Europhys. Lett. **7**, 599 (1988).
[21] M. Y. Lin, H. M. Lindsay, D. A. Weitz, R. C. Ball, R. Klein, and P. Meakin, Proc. R. Soc. London Ser. A **423**, 71 (1989).
[22] M. Y. Lin, H. M. Lindsay, D. A. Weitz, R. Klein, R. C. Ball, and P. Meakin, J. Phys. Condens. Matter **2**, 3093 (1990).
[23] M. Y. Lin, H. M. Lindsay, D. A. Weitz, R. C. Ball, R. Klein, and P. Meakin, Phys. Rev. A **41**, 2005 (1990).
[24] M. Carpineti, F. Ferri, M. Giglio, E. Paganini, and U. Perini, Phys. Rev. A **42**, 7347 (1990).
[25] J. E. Martin, J. P. Wilcoxon, D. Schaefer, and J. Odinek, Phys. Rev. A **41**, 4379 (1990).
[26] M. L. Broide and R. J. Cohen, J. Colloid Interface Sci. **153**, 493 (1992).
[27] M. Kolb and R. Jullien, J. Phys. (Paris) Lett. **45**, L977 (1984).
[28] R. Jullien and R. Botet, *Aggregation and Fractal Aggregates* (World Scientific, Singapore, 1987).
[29] A. E. González, Physica A **191**, 190 (1992).
[30] A. E. González, Phys. Rev. Lett. **71**, 2248 (1993).
[31] H. F. van Garderen *et al.*, J. Chem. Phys. **102**, 480 (1995).
[32] ST. C. Pencea and M. Dumitrascu, in *Fractal Aspects of Materials*, edited by F. Family, P. Meakin, B. Sapoval, and R. Wool (Materials Research Society, Pittsburgh, 1995), p. 373.
[33] A. E. González and G. Ramírez-Santiago, Phys. Rev. Lett. **74**, 1238 (1995).
[34] A. E. González and G. Ramírez-Santiago, J. Colloid. Interface Sci. (to be published).
[35] A. Hasmy and R. Jullien, J. Non-Cryst. Solids **186**,342 (1995).
[36] A. E. González, Phys. Rev. E **47**, 2923 (1993).
[37] D. Stauffer and A. Aharony, *Introduction to Percolation Theory* (Taylor & Francis, London, 1992).
[38] P. Meakin, T. Vicsek, and F. Family, Phys. Rev. B **31**, 564 (1985).
[39] R. C. Ball, D. A. Weitz, T. A. Witten, and F. Leyvraz, Phys. Rev. Lett. **58**, 274 (1987).